

Radial migration in galactic disks caused by resonance overlap of multiple patterns: Self-consistent simulations

I. Minchev¹, B. Famaey¹, F. Combes², P. Di Matteo³, M. Mouhcine⁴, H. Wozniak¹

¹ Observatoire Astronomique, Université de Strasbourg, CNRS UMR 7550, 67000 Strasbourg, France, e-mail: ivan.minchev@astro.unistra.fr

² Observatoire de Paris, LERMA, 61 avenue de L'Observatoire, 75014 Paris, France

³ Observatoire de Paris-Meudon, GEPI, CNRS UMR 8111, 5 pl. Jules Janssen, Meudon, 92195, France

⁴ Astrophysics Research Institute, Liverpool John Moores University, Twelve Quays House, Egerton Wharf, Birkenhead, CH41 1LD, UK

Received ...; accepted ...

ABSTRACT

We have recently identified a new radial migration mechanism resulting from the overlap of spiral and bar resonances in galactic disks. Here we confirm the efficiency of this mechanism in fully self-consistent, Tree-SPH simulations, as well as high-resolution pure N-body simulations. In all barred cases we clearly identify the effect of spiral-bar resonance overlap by a bimodality in the changes of angular momentum in the disk, ΔL , with maxima near the bar's corotation and outer Lindblad resonance. This is contrasted to the smooth distribution of ΔL for a simulation with no stable bar present, where strong radial migration is induced by multiple spirals. The presence of a disk gaseous component appears to increase the rate of angular momentum exchange by about 20%. The efficiency of this mechanism is such that galactic stellar disks can extend to over 10 scale-lengths within 1-3 Gyr in both Milky Way size and low-mass galaxies (circular velocity ~ 100 km/s). We also show that metallicity gradients can flatten in less than 1 Gyr rendering mixing in barred galaxies an order of magnitude more efficient than previously thought.

Key words. galaxies: evolution – galaxies: kinematics and dynamics – galaxies: evolution – galaxies: structure

1. Introduction

In the last decades discrepancies in the solar neighborhood age-metallicity relation have conclusively demonstrated that effective radial migration (i.e., redistribution of angular momentum) must be taking place in the Milky Way disk (Edvardsson et al. 1993; Haywood 2008; Schönrich and Binney 2009; see Minchev and Famaey 2009 for a comprehensive discussion). Until recently it was accepted that such mixing was solely caused by transient spirals (Sellwood and Binney, 2002, hereafter SB02). However, Quillen et al. (2009) showed that small satellites on radial, in-plane orbits can cause mixing in the outer disk and thus account for the fraction of low-metallicity stars present in the solar neighborhood (Haywood, 2008). Moreover, we have recently shown (Minchev and Famaey 2009, hereafter MF09) that a strong exchange of angular momentum occurs when a stellar disk is perturbed by a central bar and spiral structure (SS) simultaneously: our test-particle simulations allowed us to attribute this effect to the overlap of first and second order resonances of each perturber. Given that more than 2/3 of disk galaxies, including our own Milky Way, contain central bars, it is imperative to establish a strong understanding of the implications of this mechanism. Therefore, in this letter we study a range of fully self-consistent, Tree-SPH simulations, as well as high resolution pure N-body simulation, searching for the signature of spiral-bar coupling in the distribution of angular momentum.

2. Models and Results

While not self-consistent, test-particle simulations allow for a full control over the simulation parameters, such as the amplitudes and pattern speeds of bar and SS, and still provide a good approximation to self-consistent simulations. Employing this method in MF09, we could suppress the effect of transient spirals and thus were able to identify the non-linear effect of resonance overlap. We showed that the most important signature of this mechanism was a bimodality in the changes in angular momentum, ΔL , with maxima near the bar's corotation and its outer Lindblad resonance (OLR) regardless of the SS pattern speed. Here we analyze self-consistent simulations with strong bars and spirals, therefore mixing from both transient spirals (SB02) and resonance overlap (MF09) is expected. However, we hope to be able to identify the latter mechanism by the aforementioned bimodality, given that the distribution of ΔL of transients is more or less smooth (see SB02).

2.1. Tree-SPH simulations

With the advent of the GalMer database (<http://galmer.obspm.fr>) we are now in a position to test the predictions of MF09 by analyzing fully self-consistent simulations of isolated disk galaxies, including a gas component as well as star formation (Di Matteo et al., 2007; Chilingarian et al., 2010). Fig. 1 shows the properties of the isolated giant Sa galaxy model¹ (gSa) in GalMer. In the first row we plot stellar density contours for 5

¹ The gSa galaxy has a total mass of $2.4 \times 10^{11} M_{\text{sun}}$, a stellar disk of $9 \times 10^{10} M_{\text{sun}}$, a bulge to disk ratio of 0.25 and a gas mass

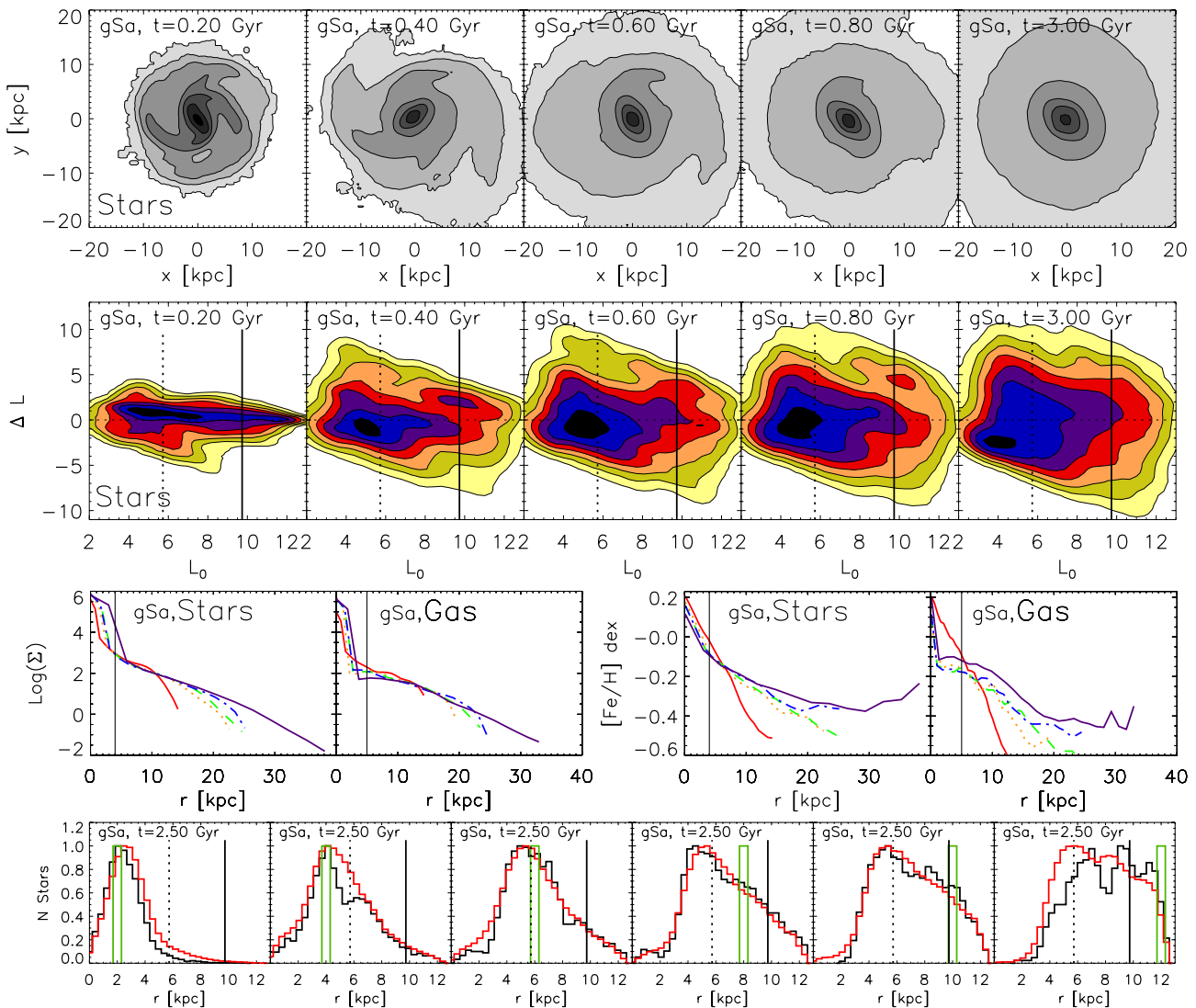


Fig. 1. First row: Stellar disk density contours of the isolated giant Sa galaxy simulation in GalMer for 5 time outputs as indicated in each panel. Second row: Changes in angular momentum, ΔL as a function of the initial angular momentum, L . Both ΔL and L are divided by the asymptotic circular velocity V_c , thus L gives approximately the galactic radius in kpc. The locations of the bar's corotation and 2:1 OLR are indicated by the dotted and solid lines, respectively. A bimodal distribution indicating the work of resonance overlap of bar and spirals is clearly seen in each panel. Third row: The evolution of the radial profiles (left) and metallicities (right) for the stellar and gaseous disks. The initial disk scale-lengths are indicated by the solid lines. The time steps shown are as in the First row, indicated by solid red, dotted orange, dashed green, dotted-dash blue and solid purple, respectively. Fourth row: Distribution of birth radii for stars ending up in the annuli indicated by the green lines (300 pc) at $t=2.5$ Gyr.

time outputs up to 3 Gyr as indicated in each panel. Note that the initially strong SS disappears by the end of the simulation. The expansion of the disk is already an indication of radial migration. The second row shows contours of the change in angular momentum of stars, ΔL , against the initial angular momentum, L_0 . Both ΔL and L are divided by the asymptotic circular velocity $V_c \approx 280$ km/s, thus L gives approximately the galactic radius in kpc. The bar's corotation and 2:1 OLR are indicated by the dotted and solid lines. A bimodal distribution becomes apparent as soon as the bar and SS form ($t \approx 0.2$ Gyr). While the peak at $L_0 \approx 4.5$ is caused by the bar's corotation, the one at $L_0 \approx 8.5$ could only be present because of resonance overlap (see Fig. 2 in MF09). At all later times there is a clear bimodality in the distribution of ΔL , thus assuring that the effect we see

equal to 0.1 times the stellar disk mass. See Sec. 2.1 and Table 1 in Chilingarian et al. (2010) for a complete description of the model.

is caused by the spiral-bar interaction. Note also that the mixing timescale here is simply too short to be the effect of transients only.

The third row of Fig. 1 shows the temporal evolution of the radial density (left) and metallicity (right) profiles for both the stellar and gaseous disks. The time steps shown are as in the first row, indicated by solid red, dotted orange, dashed green, dotted-dash blue and solid purple in an increasing order. Due to the vigorous mixing, the stellar and gaseous disks extend to about 10 and 7 scale-lengths, respectively, while roughly preserving their exponential profiles. This is accompanied by a strong flattening in the metallicity gradients, where at $t=3$ Gyr one can clearly see a reversal in the metallicity gradient of stars in the outer region of the disk (~ 30 kpc). The stellar metallicities at that location are similar to the initial ones at 8 kpc, suggesting that stars in

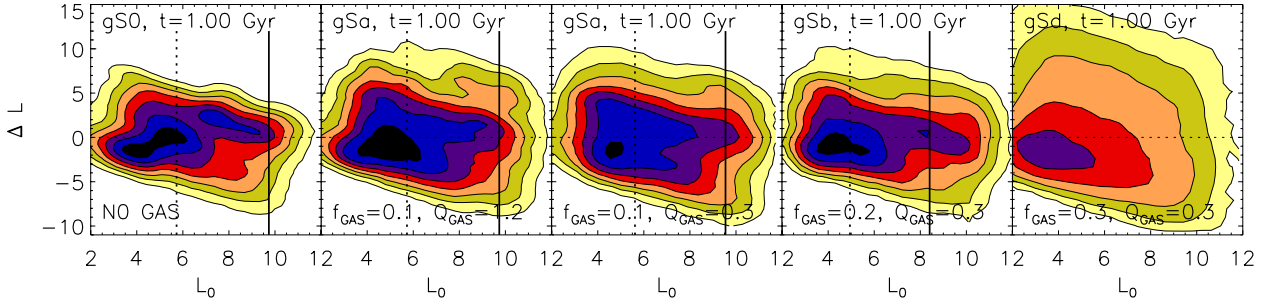


Fig. 2. Same as the second row of Fig. 1 but for all isolated giant GalMer galaxies. Contour levels are the same for all plots and the time is $t=1$ Gyr. The locations of the bar's corotation and OLR are indicated by the dotted and solid lines, respectively. The rightmost panel shows the only disk lacking a central bar. In this case resonance overlap from strong multiple spirals give rise to a smooth ΔL distribution.

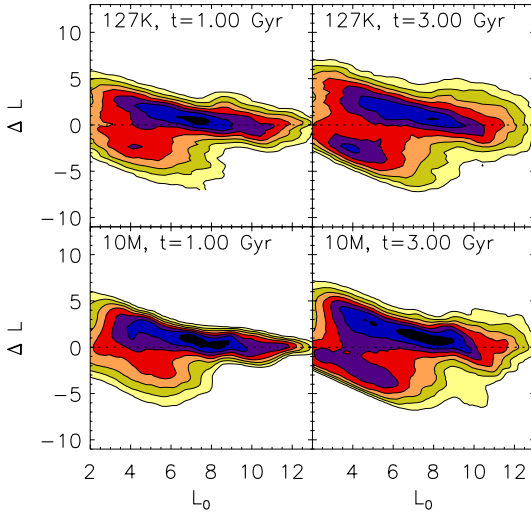


Fig. 3. Contrasting the effect on ΔL for a low-resolution (1.27×10^5) and a high-resolution 10^7 pure N-body simulations.

the outskirts of the disk originate from regions near the bar's 2:1 OLR, where the changes of ΔL are most prominent.

The bottom row of Fig. 1 shows the distribution of birth radii for stars ending up in the annuli indicated by the green lines (300 pc) at $t = 2.5$ Gyr. The black and red histograms show stars on nearly circular orbits (velocity dispersion less than 10 km/s) and the total population, respectively. In all cases there is a large fraction of stars coming from the bar's corotation (dotted line), as well as an increasingly large fraction from the bar's OLR (solid line) as larger final radii are sampled.

In Fig. 2 we plot the changes in angular momentum for the stellar disk components of all GalMer isolated giant galaxy models available. Contour levels are the same for all plots and the time is $t=1$ Gyr. All but the gSd (bulgeless) model develop long-lived, central bars at the beginning of the simulation and consequently show a bimodality in ΔL . When comparing the gS0 and gSa models, which have identical initial conditions but gS0 is gas-free, we observe that $\sim 20\%$ increase in the effect on ΔL is seen when a gaseous disk component is present. The stability of the gas appears not to play a major role, however. There is indeed only a small difference when the gas is made more unstable by lowering Q_{gas} from 1.2 to 0.3 (second and third panels), where Q_{gas} is the Toomre instability parameter for the gas. The weaker bar in the gSb model (fourth panel) results in a reduced mixing as we predicted in MF09. Unlike all other models, the gSd simulation (rightmost panel) does not form a stable bar.

The strong mixing observed here results from the large number of multiple spirals (Elmegreen et al., 1992; Rix and Rieke, 1993; Minchev and Quillen, 2006) propagating simultaneously through the disk during the first ~ 500 Myr. Due to the various SS pattern speeds, there are no radii at which the effect of resonance overlap is distinctly different from the rest of the disk (such as the bar's corotation and OLR). Consequently, we observe a smooth distribution of ΔL in contrast to the case of bar + SS.

2.2. High resolution N-body simulations

To determine whether the strong mixing we described above is caused by deficiency in the resolution of GalMer simulations, we ran pure N-body collisionless simulations with 10^7 and 1.27×10^5 particles in the disk. Full description and details can be found in Wozniak and Michel-Dansac (2009). With a scale-length of 3.5 kpc, the initial conditions of the disk are comparable to the gSb GalMer model (Fig. 2) but without a gas component. These simulations have no halo which results in a $\sim 30\%$ drop of the RC at ~ 10 kpc.

Fig. 3 shows the changes in angular momentum at $t=1$ and 3 Gyr for 1.27×10^5 (top) and 10^7 (bottom) disk particles. At the beginning of the simulations the effect is stronger for the low-resolution case due to the faster bar formation. However, at $t \approx 2$ Gyr both the high- and low-resolution runs yield a similar result. This suggests that the magnitude of the radial migration induced by the bar-spiral interaction and the timescale over which it is effective are not strongly dependent on the numerical resolution of the simulations. We conclude that the properties of the mixing, i.e., its magnitude and timescale, we infer from the GalMer simulations are only weakly affected by the insufficient resolution.

2.3. Migration in low-mass galaxies

Is the resonance overlap mechanism also efficient in low-mass galaxies? Gogarten et al. (2010) have shown that although transient spirals can explain extended disks for MW-type galaxies, this mixing mechanism is inefficient for galaxies with RCs of $V_c \sim 100$ km/s. We now consider the barred, dwarf Sa (dSa) simulation in GalMer (RC of 100 km/s and initial scale-length of 1.3 kpc) to see how its density distribution and metallicity gradient evolve with time. In Fig. 4 we plot the time development of the stellar disk density and metallicity profiles, for the same time steps as in Fig. 1. We can clearly see that the stellar disk extends to more than 10 scale-lengths in ~ 3 Gyr, while preserving

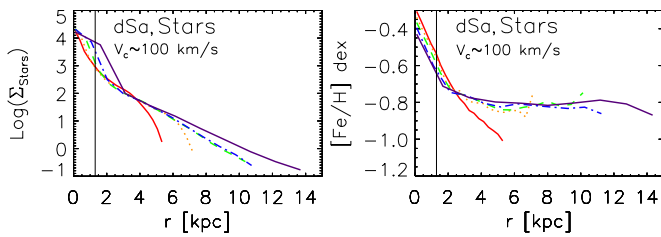


Fig. 4. The time evolution of the stellar disk density (left) and metallicity (right) profiles for the dwarf Sa isolated GalMer model. Time outputs and colors are the same as the third row of Fig. 1. This is a low-mass galaxy with a rotation curve of ~ 100 km/s similar to NGC 300 and M33. The initial disk scale-length is indicated by the solid line. The disk extends to over 10 scale-lengths in less than 3 Gyr.

an exponential profile. At the same time the metallicity gradient becomes flat in less than 1 Gyr. Both the predicted extent of the stellar disk and the flattening of the metallicity profile are consistent with what has been recently reported for nearby low-mass galaxies (Bland-Hawthorn et al., 2005; Vlajić et al., 2009).

3. Conclusions

We have examined the redistribution of angular momentum in galactic disks by means of Tree-SPH and high-resolution pure N-body simulations. We have found that resonance overlap of bar + SS or SS + SS induces strong exchange of angular momentum throughout the disks in agreement with the predictions of Minchev and Famaey (2009). Since in the self-consistent simulations analyzed in this work spirals are transient, we should also expect contribution from the SB02 radial migration mechanism. However, for the short timescales considered here (< 1 Gyr) transients would simply have a very small effect (SB02). The resonance overlap mechanism is clearly identified by a bimodality in the changes in angular momentum, ΔL , caused by the bar's corotation and 2:1 OLR (Fig. 1, 2, and 3). We have contrasted this to a simulation lacking a stable central bar (Fig. 2, right-most panel), where the ΔL distribution is smooth. The effect is especially strong when a gaseous component is present due to the exchange of L between gas and stars coming from the gravity torques, the phase shift between the two components, and the gas dissipation (Bournaud and Combes, 2002). Depending on the amount of gas and strength of bars and spirals, metallicity gradients can flatten in less than 1 Gyr (Fig. 1). This is in drastic contrast to the current understanding that galactic disks need a Hubble time for sufficient mixing (SB02, Roškar et al. 2008).

How can we tie our results to galactic disk evolution? Bournaud and Combes (2002) followed the detailed processes of bar formation, bar destruction and bar re-formation, while varying the disk to bulge ratio. These authors identified three such bar formation episodes in a Hubble time. In this model we can regard a given GalMer isolated galaxy simulation as one such episode of a gas accretion event during a galaxy lifetime. In this scenario the fast flattening in the metallicity gradients expected from the vigorous migration (Fig. 1) would be followed by a gas enrichment at each bar re-formation event resulting in rebuilding the gradient. The presence or not of a metallicity gradient, or its intensity, would then be an indicator of the bar/accretion phase of the galaxy.

The mechanism described in this study works even in low-mass galaxies (Fig. 4) and can thus provide an explanation for the extended disk profiles observed in galaxies with $V_c \sim$

100 km/s (Bland-Hawthorn et al., 2005). A future work is dedicated to this problem (Minchev et al. 2010, In preparation).

Acknowledgements. Support for this work was provided by ANR and RAVE.

References

- Bland-Hawthorn, J., Vlajić, M., Freeman, K. C., and Draine, B. T.: 2005, *ApJ* **629**, 239
- Bournaud, F. and Combes, F.: 2002, *A&A* **392**, 83
- Chilingarian, I., Di Matteo, P., Combes, F., Melchior, A., and Semelin, B.: 2010, *ArXiv e-prints*
- Di Matteo, P., Combes, F., Melchior, A., and Semelin, B.: 2007, *A&A* **468**, 61
- Edvardsson, B.: 1993, *A&A* **275**, 101
- Elmegreen, B. G., Elmegreen, D. M., and Montenegro, L.: 1992, *ApJS* **79**, 37
- Gogarten, S. M.: 2010, *ApJ* **712**, 858
- Haywood, M.: 2008, *MNRAS* **388**, 1175
- Minchev, I. and Famaey, B.: 2009, *arXiv:0911.1794v1*
- Minchev, I. and Quillen, A. C.: 2006, *MNRAS* **368**, 623
- Quillen, A. C., Minchev, I., Bland-Hawthorn, J., and Haywood, M.: 2009, *MNRAS* **397**, 1599
- Rix, H. and Rieke, M. J.: 1993, *ApJ* **418**, 123
- Roškar, R., Debattista, V. P., Quinn, T. R., Stinson, G. S., and Wadsley, J.: 2008, *ApJ* **684**, L79
- Schönrich, R. and Binney, J.: 2009, *MNRAS* **396**, 203
- Sellwood, J. A. and Binney, J. J.: 2002, *MNRAS* **336**, 785
- Vlajić, M., Bland-Hawthorn, J., and Freeman, K. C.: 2009, *ApJ* **697**, 361
- Wozniak, H. and Michel-Dansac, L.: 2009, *A&A* **494**, 11